

Proceedings of the 12<sup>th</sup> International Conference on  
Computational Fluid Dynamics in the Oil & Gas,  
Metallurgical and Process Industries

# Progress in Applied CFD – CFD2017



SINTEF Proceedings

Editors:

Jan Erik Olsen and Stein Tore Johansen

## **Progress in Applied CFD – CFD2017**

Proceedings of the 12<sup>th</sup> International Conference on Computational Fluid Dynamics  
in the Oil & Gas, Metallurgical and Process Industries

SINTEF Academic Press

SINTEF Proceedings no 2

Editors: Jan Erik Olsen and Stein Tore Johansen

**Progress in Applied CFD – CFD2017**

Selected papers from 10<sup>th</sup> International Conference on Computational Fluid Dynamics in the Oil & Gas, Metallurgical and Process Industries

Key words:

CFD, Flow, Modelling

Cover, illustration: Arun Kamath

ISSN 2387-4295 (online)

ISBN 978-82-536-1544-8 (pdf)

© Copyright SINTEF Academic Press 2017

The material in this publication is covered by the provisions of the Norwegian Copyright Act. Without any special agreement with SINTEF Academic Press, any copying and making available of the material is only allowed to the extent that this is permitted by law or allowed through an agreement with Kopinor, the Reproduction Rights Organisation for Norway. Any use contrary to legislation or an agreement may lead to a liability for damages and confiscation, and may be punished by fines or imprisonment

SINTEF Academic Press

Address:       Forskningsveien 3 B  
                  PO Box 124 Blindern  
                  N-0314 OSLO

Tel:             +47 73 59 30 00

Fax:            +47 22 96 55 08

[www.sintef.no/byggforsk](http://www.sintef.no/byggforsk)

[www.sintefbok.no](http://www.sintefbok.no)

**SINTEF Proceedings**

SINTEF Proceedings is a serial publication for peer-reviewed conference proceedings on a variety of scientific topics.

The processes of peer-reviewing of papers published in SINTEF Proceedings are administered by the conference organizers and proceedings editors. Detailed procedures will vary according to custom and practice in each scientific community.

## PREFACE

This book contains all manuscripts approved by the reviewers and the organizing committee of the 12th International Conference on Computational Fluid Dynamics in the Oil & Gas, Metallurgical and Process Industries. The conference was hosted by SINTEF in Trondheim in May/June 2017 and is also known as CFD2017 for short. The conference series was initiated by CSIRO and Phil Schwarz in 1997. So far the conference has been alternating between CSIRO in Melbourne and SINTEF in Trondheim. The conferences focuses on the application of CFD in the oil and gas industries, metal production, mineral processing, power generation, chemicals and other process industries. In addition pragmatic modelling concepts and bio-mechanical applications have become an important part of the conference. The papers in this book demonstrate the current progress in applied CFD.

The conference papers undergo a review process involving two experts. Only papers accepted by the reviewers are included in the proceedings. 108 contributions were presented at the conference together with six keynote presentations. A majority of these contributions are presented by their manuscript in this collection (a few were granted to present without an accompanying manuscript).

The organizing committee would like to thank everyone who has helped with review of manuscripts, all those who helped to promote the conference and all authors who have submitted scientific contributions. We are also grateful for the support from the conference sponsors: ANSYS, SFI Metal Production and NanoSim.

Stein Tore Johansen & Jan Erik Olsen



Organizing committee:

Conference chairman: Prof. Stein Tore Johansen

Conference coordinator: Dr. Jan Erik Olsen

Dr. Bernhard Müller

Dr. Sigrid Karstad Dahl

Dr. Shahriar Amini

Dr. Ernst Meese

Dr. Josip Zoric

Dr. Jannike Solsvik

Dr. Peter Witt

Scientific committee:

Stein Tore Johansen, SINTEF/NTNU

Bernhard Müller, NTNU

Phil Schwarz, CSIRO

Akio Tomiyama, Kobe University

Hans Kuipers, Eindhoven University of Technology

Jinghai Li, Chinese Academy of Science

Markus Braun, Ansys

Simon Lo, CD-adapco

Patrick Segers, Universiteit Gent

Jiyuan Tu, RMIT

Jos Derksen, University of Aberdeen

Dmitry Eskin, Schlumberger-Doll Research

Pär Jönsson, KTH

Stefan Pirker, Johannes Kepler University

Josip Zoric, SINTEF

## CONTENTS

<b>PRAGMATIC MODELLING .....</b>	<b>9</b>
On pragmatism in industrial modeling. Part III: Application to operational drilling .....	11
CFD modeling of dynamic emulsion stability .....	23
Modelling of interaction between turbines and terrain wakes using pragmatic approach .....	29
<b>FLUIDIZED BED .....</b>	<b>37</b>
Simulation of chemical looping combustion process in a double looping fluidized bed reactor with cu-based oxygen carriers.....	39
Extremely fast simulations of heat transfer in fluidized beds.....	47
Mass transfer phenomena in fluidized beds with horizontally immersed membranes .....	53
A Two-Fluid model study of hydrogen production via water gas shift in fluidized bed membrane reactors .....	63
Effect of lift force on dense gas-fluidized beds of non-spherical particles .....	71
Experimental and numerical investigation of a bubbling dense gas-solid fluidized bed .....	81
Direct numerical simulation of the effective drag in gas-liquid-solid systems .....	89
A Lagrangian-Eulerian hybrid model for the simulation of direct reduction of iron ore in fluidized beds.....	97
High temperature fluidization - influence of inter-particle forces on fluidization behavior .....	107
Verification of filtered two fluid models for reactive gas-solid flows .....	115
<b>BIOMECHANICS.....</b>	<b>123</b>
A computational framework involving CFD and data mining tools for analyzing disease in carotid artery .....	125
Investigating the numerical parameter space for a stenosed patient-specific internal carotid artery model.....	133
Velocity profiles in a 2D model of the left ventricular outflow tract, pathological case study using PIV and CFD modeling.....	139
Oscillatory flow and mass transport in a coronary artery.....	147
Patient specific numerical simulation of flow in the human upper airways for assessing the effect of nasal surgery.....	153
CFD simulations of turbulent flow in the human upper airways .....	163
<b>OIL &amp; GAS APPLICATIONS .....</b>	<b>169</b>
Estimation of flow rates and parameters in two-phase stratified and slug flow by an ensemble Kalman filter .....	171
Direct numerical simulation of proppant transport in a narrow channel for hydraulic fracturing application .....	179
Multiphase direct numerical simulations (DNS) of oil-water flows through homogeneous porous rocks .....	185
CFD erosion modelling of blind tees .....	191
Shape factors inclusion in a one-dimensional, transient two-fluid model for stratified and slug flow simulations in pipes .....	201
Gas-liquid two-phase flow behavior in terrain-inclined pipelines for wet natural gas transportation .....	207

<b>NUMERICS, METHODS &amp; CODE DEVELOPMENT .....</b>	<b>213</b>
Innovative computing for industrially-relevant multiphase flows .....	215
Development of GPU parallel multiphase flow solver for turbulent slurry flows in cyclone.....	223
Immersed boundary method for the compressible Navier–Stokes equations using high order summation-by-parts difference operators .....	233
Direct numerical simulation of coupled heat and mass transfer in fluid-solid systems .....	243
A simulation concept for generic simulation of multi-material flow, using staggered Cartesian grids.....	253
A cartesian cut-cell method, based on formal volume averaging of mass, momentum equations.....	265
SOFT: a framework for semantic interoperability of scientific software .....	273
<b>POPULATION BALANCE .....</b>	<b>279</b>
Combined multifluid-population balance method for polydisperse multiphase flows .....	281
A multifluid-PBE model for a slurry bubble column with bubble size dependent velocity, weight fractions and temperature.....	285
CFD simulation of the droplet size distribution of liquid-liquid emulsions in stirred tank reactors .....	295
Towards a CFD model for boiling flows: validation of QMOM predictions with TOPFLOW experiments .....	301
Numerical simulations of turbulent liquid-liquid dispersions with quadrature-based moment methods.....	309
Simulation of dispersion of immiscible fluids in a turbulent couette flow .....	317
Simulation of gas-liquid flows in separators - a Lagrangian approach.....	325
CFD modelling to predict mass transfer in pulsed sieve plate extraction columns .....	335
<b>BREAKUP &amp; COALESCENCE .....</b>	<b>343</b>
Experimental and numerical study on single droplet breakage in turbulent flow .....	345
Improved collision modelling for liquid metal droplets in a copper slag cleaning process .....	355
Modelling of bubble dynamics in slag during its hot stage engineering.....	365
Controlled coalescence with local front reconstruction method .....	373
<b>BUBBLY FLOWS .....</b>	<b>381</b>
Modelling of fluid dynamics, mass transfer and chemical reaction in bubbly flows .....	383
Stochastic DSMC model for large scale dense bubbly flows.....	391
On the surfacing mechanism of bubble plumes from subsea gas release.....	399
Bubble generated turbulence in two fluid simulation of bubbly flow .....	405
<b>HEAT TRANSFER .....</b>	<b>413</b>
CFD-simulation of boiling in a heated pipe including flow pattern transitions using a multi-field concept .....	415
The pear-shaped fate of an ice melting front .....	423
Flow dynamics studies for flexible operation of continuous casters (flow flex cc).....	431
An Euler-Euler model for gas-liquid flows in a coil wound heat exchanger.....	441
<b>NON-NEWTONIAN FLOWS.....</b>	<b>449</b>
Viscoelastic flow simulations in disordered porous media .....	451
Tire rubber extrudate swell simulation and verification with experiments .....	459
Front-tracking simulations of bubbles rising in non-Newtonian fluids.....	469
A 2D sediment bed morphodynamics model for turbulent, non-Newtonian, particle-loaded flows.....	479

<b>METALLURGICAL APPLICATIONS.....</b>	<b>491</b>
Experimental modelling of metallurgical processes .....	493
State of the art: macroscopic modelling approaches for the description of multiphysics phenomena within the electroslag remelting process .....	499
LES-VOF simulation of turbulent interfacial flow in the continuous casting mold .....	507
CFD-DEM modelling of blast furnace tapping .....	515
Multiphase flow modelling of furnace tapholes .....	521
Numerical predictions of the shape and size of the raceway zone in a blast furnace.....	531
Modelling and measurements in the aluminium industry - Where are the obstacles? .....	541
Modelling of chemical reactions in metallurgical processes.....	549
Using CFD analysis to optimise top submerged lance furnace geometries .....	555
Numerical analysis of the temperature distribution in a martensic stainless steel strip during hardening.....	565
Validation of a rapid slag viscosity measurement by CFD.....	575
Solidification modeling with user defined function in ANSYS Fluent.....	583
Cleaning of polycyclic aromatic hydrocarbons (PAH) obtained from ferroalloys plant.....	587
Granular flow described by fictitious fluids: a suitable methodology for process simulations .....	593
A multiscale numerical approach of the dripping slag in the coke bed zone of a pilot scale Si-Mn furnace.....	599
<b>INDUSTRIAL APPLICATIONS .....</b>	<b>605</b>
Use of CFD as a design tool for a phosphoric acid plant cooling pond .....	607
Numerical evaluation of co-firing solid recovered fuel with petroleum coke in a cement rotary kiln: Influence of fuel moisture .....	613
Experimental and CFD investigation of fractal distributor on a novel plate and frame ion-exchanger .....	621
<b>COMBUSTION .....</b>	<b>631</b>
CFD modeling of a commercial-size circle-draft biomass gasifier.....	633
Numerical study of coal particle gasification up to Reynolds numbers of 1000.....	641
Modelling combustion of pulverized coal and alternative carbon materials in the blast furnace raceway .....	647
Combustion chamber scaling for energy recovery from furnace process gas: waste to value .....	657
<b>PACKED BED.....</b>	<b>665</b>
Comparison of particle-resolved direct numerical simulation and 1D modelling of catalytic reactions in a packed bed .....	667
Numerical investigation of particle types influence on packed bed adsorber behaviour .....	675
CFD based study of dense medium drum separation processes .....	683
A multi-domain 1D particle-reactor model for packed bed reactor applications.....	689
<b>SPECIES TRANSPORT &amp; INTERFACES .....</b>	<b>699</b>
Modelling and numerical simulation of surface active species transport - reaction in welding processes .....	701
Multiscale approach to fully resolved boundary layers using adaptive grids.....	709
Implementation, demonstration and validation of a user-defined wall function for direct precipitation fouling in Ansys Fluent.....	717



<b>FREE SURFACE FLOW &amp; WAVES .....</b>	<b>727</b>
Unresolved CFD-DEM in environmental engineering: submarine slope stability and other applications.....	729
Influence of the upstream cylinder and wave breaking point on the breaking wave forces on the downstream cylinder .....	735
Recent developments for the computation of the necessary submergence of pump intakes with free surfaces .....	743
Parallel multiphase flow software for solving the Navier-Stokes equations .....	752
 <b>PARTICLE METHODS .....</b>	 <b>759</b>
A numerical approach to model aggregate restructuring in shear flow using DEM in Lattice-Boltzmann simulations .....	761
Adaptive coarse-graining for large-scale DEM simulations.....	773
Novel efficient hybrid-DEM collision integration scheme.....	779
Implementing the kinetic theory of granular flows into the Lagrangian dense discrete phase model.....	785
Importance of the different fluid forces on particle dispersion in fluid phase resonance mixers .....	791
Large scale modelling of bubble formation and growth in a supersaturated liquid.....	798
 <b>FUNDAMENTAL FLUID DYNAMICS .....</b>	 <b>807</b>
Flow past a yawed cylinder of finite length using a fictitious domain method .....	809
A numerical evaluation of the effect of the electro-magnetic force on bubble flow in aluminium smelting process.....	819
A DNS study of droplet spreading and penetration on a porous medium.....	825
From linear to nonlinear: Transient growth in confined magnetohydrodynamic flows.....	831

## A TWO-FLUID MODEL STUDY OF HYDROGEN PRODUCTION VIA WATER GAS SHIFT IN FLUIDIZED BED MEMBRANE REACTORS

Ramon J.W. VONCKEN<sup>1</sup>, Ivo ROGHAI<sup>1\*</sup>, Martin VAN SINT ANNALAND<sup>1</sup>

<sup>1</sup> Chemical Process Intensification, Department of Chemical Engineering and Chemistry, Eindhoven University of Technology, THE NETHERLANDS

\* Corresponding author e-mail: i.roghair@tue.nl

### ABSTRACT

Fluidized bed membrane reactors have been proposed as a promising reactor concept for the production of ultra-pure hydrogen via Water Gas Shift (WGS). High-flux thin-film dense palladium-based membranes are used to selectively extract hydrogen from the reaction medium, which shifts the thermodynamic equilibrium towards the products' side, increasing the conversion. A Two-Fluid Model (TFM) has been used to investigate the effect of hydrogen extraction via perm-selective membranes on the WGS reaction rates in the fluidized bed. A thorough TFM verification study was performed, which showed that the model is able to accurately predict the concentration profiles for various types of  $n^{\text{th}}$  order and equilibrium chemical reactions. Also, the implementation of the WGS reaction rate in the TFM was checked. The results have shown a clear positive effect of the hydrogen permeation on the WGS reaction rates, both for vertically and horizontally immersed membranes. In systems with horizontally immersed membranes, gas pockets that contain a very small amount of catalyst develop underneath the membrane tube, resulting in reduced local reaction rates. Densified zones on top of the membrane tube show increased local reaction rates. Mass transfer limitations from the emulsion phase to the membrane surface is the most pronounced effect that reduces the overall reactor performance. The developed model allows further investigating different configurations and operation modes to further optimize the reactor's performance.

**Keywords:** Two-Fluid Model, Water Gas Shift, hydrogen, fluidized bed, membrane.

### NOMENCLATURE

#### Latin Symbols

$A$	area	[m <sup>2</sup> ]
$A_{WGS}$	pre-factor WGS reaction rate	[mol/(bar kg <sub>cat</sub> s)]
$B_{WGS}$	Relative equilibrium ratio eq.	[-]
$C_d$	drag coefficient	[-]
$C_1$	constant for Gibbs calc.	[J/(mol K <sup>3</sup> )]
$C_2$	constant for Gibbs calc.	[J/(mol K <sup>2</sup> )]
$C_3$	constant for Gibbs calc.	[J/(mol K)]
$C_4$	constant for Gibbs calc.	[J/mol]
$D$	diffusion coefficient	[m <sup>2</sup> /s]
$E_{act}$	Activation energy	[J/mol]
$e$	restitution coefficient	[-]

$G$	Gibbs free energy	[J/mol]
$H$	enthalpy	[J/mol]
$g$	gravitational acceleration	[m/s <sup>2</sup> ]
$k_{WGS}$	WGS reaction rate constant	[mol/(bar kg <sub>cat</sub> s)]
$K_{eq,WGS}$	WGS equilibrium constant	[-]
$M$	molar weight	[kg/mol]
$n$	power in Sieverts' law	[-]
$p$	pressure	[Pa]
$P$	partial pressure	[Pa]
$Q$	membrane permeance	[mol/(m <sup>2</sup> s Pa <sup>n</sup> )]
$R$	universal gas constant	[J/(mol.K)]
$R_{WGS}$	chemical reaction rate	[mol/(kg <sub>cat</sub> s)]
$Re$	Reynolds number	[-]
$S$	membrane mass source term	[kg/(m <sup>3</sup> .s)]
$t$	time	[s]
$T$	temperature	[K]
$u$	velocity	[m/s]
$V$	volume	[m <sup>3</sup> ]
$X$	molar fraction	[-]
$Y$	mass fraction	[-]

#### Greek Symbols

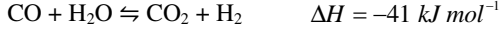
$\alpha$	hold-up fraction	[-]
$\beta$	interphase drag coefficient	[kg/(m <sup>3</sup> s)]
$\gamma$	dissipation of fluct. energy	[kg/(m s <sup>3</sup> )]
$\theta$	granular temperature	[m <sup>2</sup> /s <sup>2</sup> ]
$\kappa$	conductivity of fluct. energy	[kg/(m s)]
$\mu$	shear/dynamic viscosity	[Pa.s]
$\rho$	density	[kg/m <sup>3</sup> ]
$\tau$	shear stress tensor	[N/m <sup>2</sup> ]
$\omega_{cat}$	catalyst mass fraction	[-]

#### Sub/superscripts

$c$	cell
$g$	gas
$i$	phase
$m$	membrane
$mf$	minimum fluidization
$p$	particle
$ret$	retentate
$s$	solid
$sim$	simulation
$tot$	total
$w$	wall

## INTRODUCTION

Hydrogen is industrially mostly produced via Steam Methane Reforming (SMR) carried out in multi-tubular packed bed reactors. First, methane reacts with steam to form carbon monoxide and hydrogen at temperatures around 1000 °C. Consecutively, the formed carbon monoxide reacts with steam to form carbon dioxide and hydrogen via the Water Gas Shift (WGS) reaction, given by



WGS is thermodynamically favoured at low temperatures and kinetically favoured at higher temperatures. Traditionally, WGS reactors consist of two stages; in the first reactor most of the CO is converted at 300-450 °C and in the second reactor the remaining CO is converted at 200-300 °C. However, to produce hydrogen efficiently, low hydrogen concentrations are required to achieve high CO conversions. Costly and energy intensive separation units, such as pressure swing adsorption units, are required to separate the hydrogen from the outlet gas mixture. The process will have an additional cost and energy penalty, if the unwanted byproduct CO<sub>2</sub> should be separated from the gas mixture and stored underground (Medrano et al. (2014)).

Both packed bed membrane reactors (Tiemersma et al. (2006)) and fluidized bed membrane reactors (Fernandez et al. (2015)) have been proposed as alternative reactor systems for hydrogen production via WGS. This work will focus on the development of fluidized bed membrane reactors (FBMRs) for hydrogen production via WGS. In FBMRs, the reaction and separation steps have been integrated in one single unit; ultra-pure hydrogen is obtained from the reactor by extracting it from the gas mixture with modern high-flux hydrogen perm-selective supported palladium-based membranes. The hydrogen extraction drives the reaction equilibrium towards the products' side, which will increase the reaction rate and reactant conversion. The WGS reaction is highly suitable for hydrogen production in an FBMR, because hydrogen can be produced at 400 °C, high enough to avoid problems associated with membrane embrittlement and low enough to circumvent problems related to the membrane chemical/mechanical stability and membrane sealing.

Fluidized bed membrane reactors have already been investigated by a.o. Adris et al. (1994), Gallucci (2008) and Mleczko et al. (1996), and many others. Most of the previous fluidized bed membrane reactor studies were either focused on experimental demonstration or using phenomenological models. More recently, various CFD studies on fluidized bed membrane reactors have been performed, which have mostly investigated the bed hydrodynamics (De Jong et al. (2012), Tan et al. (2014) and Medrano et al. (2015)). Only a few studies have investigated FBMRs with CFD models focused on mass transfer phenomena and chemical reactions (e.g. Hommel et al. (2012), Voncken et al. (2015) and Helmi et al. (2017)).

The present work uses CFD simulations to visualize and quantify the mass transfer phenomena and reaction rates throughout FBMR systems in which hydrogen is produced via WGS. The OpenFOAM v.2.3.0 solver *twoPhaseEulerFoam*, a Two-Fluid Model (TFM), was used to model hydrodynamics, mass transfer and chemical reactions occurring in various fluidized bed membrane reactor configurations. The chemical species balances, selective membrane extraction and chemical reactions are our own implementations that were coupled to the TFM hydrodynamics. A thorough verification was carried out for all these aspects. To ensure the reaction terms have been implemented properly, numerous simple chemical reactions in a batch reactor have been simulated and compared to analytical and numerical solutions. The more complex kinetics of the WGS reaction have also been implemented in the TFM and compared to a batch reactor model.

The objective of this research is to understand and quantify the effect of selective hydrogen permeation on the performance of fluidized bed reactors for hydrogen production via WGS. The Numaguchi and Kikuchi (1988) reaction kinetics for WGS were implemented in the TFM. Both horizontally and vertically immersed membrane configurations were studied. These results were compared to the performance of a fluidized bed reactor without membranes.

First, the model equations and the verification of their implementation will be discussed. Special attention will be given to the species balance and the reaction kinetics. Next, the used simulation settings and geometries will be presented. In the results section, the effect of the extraction via the membranes on the reaction rates and reactor performance will be discussed.

## MODEL DESCRIPTION

The TFM considers the gas and solids phases as interpenetrating continua. The most important governing and constitutive equations are presented in equations 1 through 4, showing the continuity and Navier-Stokes equations of both the gas and solids phases. The source term  $S$  is added to the gas continuity equation to account for the extraction of gas via the membranes, which will be detailed later. The gas phase is considered as an ideal, Newtonian fluid. The solids phase rheology (solids pressure  $p_s$  and stress tensor  $\boldsymbol{\tau}_s$  is described with closures from the Kinetic Theory of Granular Flow, for which the granular temperature equation (4) is solved.

$$\frac{\partial(\alpha_i \rho_i)}{\partial t} + \nabla \cdot (\alpha_i \rho_i \mathbf{u}_i) = S_m, \quad i = s, g \quad (1)$$

$$\begin{aligned} & \frac{\partial(\alpha_g \rho_g \mathbf{u}_g)}{\partial t} + \nabla \cdot (\alpha_g \rho_g \mathbf{u}_g \mathbf{u}_g) \\ & = -\nabla \cdot (\alpha_g \boldsymbol{\tau}_g) - \alpha_g \nabla p - \beta (\mathbf{u}_g - \mathbf{u}_s) + \alpha_g \rho_g \mathbf{g} \end{aligned} \quad (2)$$

$$\begin{aligned} & \frac{\partial(\alpha_s \rho_s \mathbf{u}_s)}{\partial t} + \nabla \cdot (\alpha_s \rho_s \mathbf{u}_s \mathbf{u}_s) = -\nabla \cdot (\alpha_s \boldsymbol{\tau}_s) \\ & - \alpha_s \nabla p - \nabla p_s + \beta (\mathbf{u}_g - \mathbf{u}_s) + \alpha_s \rho_s \mathbf{g} \end{aligned} \quad (3)$$

$$\frac{3}{2} \left( \frac{\partial(\alpha_s \rho_s \theta)}{\partial t} + \nabla \times (\alpha_s \rho_s \mathbf{u}_s \theta) \right) = -\gamma_s - 3\beta\theta \quad (4)$$

$$-(p_s \mathbf{I} + \alpha_s \boldsymbol{\tau}_s) : \nabla \mathbf{u}_s + \nabla \times (\alpha_s \kappa_s \nabla \theta)$$

The fluid-particle drag is modelled according to Gidaspow (1994), which combines the drag models by Ergun et al. (1949) and Wen et al. (1966), where Ergun's model is valid for high solids hold-ups (above 20%) and Wen's model is applied at lower solids hold-ups (below 20%). The drag coefficient  $C_d$  is determined based on the Reynolds particle number. The drag models are described in equations 5 until 9.

$$\beta = 150 \frac{\alpha_s^2 \mu_g}{\alpha_g d_p^2} + 1.75 \frac{\alpha_s \rho_g |\mathbf{u}_g - \mathbf{u}_s|}{d_p} \quad (\alpha_s \geq 0.20) \quad (5)$$

$$\beta = \frac{3}{4} C_d \frac{\alpha_g \alpha_s \rho_g}{d_p} |\mathbf{u}_g - \mathbf{u}_s| \alpha_g^{-2.65} \quad (\alpha_s < 0.20) \quad (6)$$

$$C_d = \frac{24}{\text{Re}_p} (1 + 0.15 \text{Re}_p^{0.687}) \quad \text{for } \text{Re}_p \leq 1000 \quad (7)$$

$$C_d = 0.44 \quad \text{for } \text{Re}_p > 1000 \quad (8)$$

$$\text{Re}_p = \alpha_g \frac{\rho_g d_p |\mathbf{u}_g - \mathbf{u}_s|}{\mu_g} \quad (9)$$

### Kinetic Theory of Granular Flow

To simulate the rheological properties of the solids phase's continuum approximation, various KTGF closure equations are required. The closure equations used in this work are summarized in **Table 1**.

**Table 1:** KTGF closures used for TFM simulations.

Quantity	Closure
Solids shear viscosity	Nieuwland et al. (1996)
Solids bulk viscosity	Lun et al. (1984)
Solids pressure	Lun et al. (1984)
Frictional stress	Srivastava & Sundaresan (2003)
Conductivity of fluct. energy	Nieuwland et al. (1996)
Radial distribution function	Ma & Ahmadi (1984)
Dissipation of gran. energy	Nieuwland et al. (1996)

Further details on the TFM-KTGF can be found a.o. in Lun et al. (1984), Kuipers et al. (1992), Gidaspow (1994), Van Wachem (2000), Rusche (2003) and Van Der Hoef et al. (2006). Details on the OpenFOAM TFM can be found in Passalacqua et al. (2011) and Liu et al. (2014).

### Mass transfer, membranes and reactions

Mass transfer phenomena and extraction of hydrogen via membranes were modeled with an approach similar to that described by Coroneo et al. (2009), see equation 10. Extraction of hydrogen via the membranes was modeled via source term,  $S_m$ , to the species equation of hydrogen. This membrane source term is applied to the

computational cells adjacent to a membrane. The membrane source term is calculated with Sieverts' law, which is commonly used to describe the hydrogen flux through dense palladium membranes (see equation 11). The parameters in Sieverts' law are obtained from experiments. The extraction of mass via a membrane will also result in momentum extraction from the system. Therefore, a boundary condition was added for the membranes to ensure momentum leaves the system via the membranes, see equation 12.

$$\frac{\partial \alpha_g \rho_g Y_i}{\partial t} + \nabla \times (\alpha_g \rho_g \mathbf{u}_g Y_i) \quad (10)$$

$$= \nabla \times (\alpha_g \rho_g D_i \nabla Y_i) + S_m + R_i$$

$$S_m = \frac{A_c}{V_c} Q_m M_{H_2} \times \left[ (X_{H_2}^{ret} p_{tot})^n - (X_{H_2}^{perm} p_{tot})^n \right] \quad (11)$$

$$u_m = \frac{S_m RT}{p M_{H_2} A_c} \quad (12)$$

The Numaguchi and Kikuchi (1988) kinetics for the WGS reaction were implemented in the TFM model. The reaction rate equation and their corresponding parameters (reaction rate constants, pre-factors, equilibrium constants) are presented in **Table 2** and **Table 3**.

**Table 2:** Chemical reaction rates for WGS.

$$R_{WGS} = k_{WGS} \frac{P_{CO} P_{H_2O} - \frac{P_{CO_2} P_{H_2}}{K_{eq,WGS}}}{P_{H_2O}}$$

$$k_{WGS} = A_{WGS} \exp\left(-\frac{E_{act}}{RT}\right)$$

$$K_{eq,WGS} = \exp\left(\frac{-\Delta G_{WGS}}{RT}\right)$$

$$\Delta G_{WGS} = C_1 T^3 + C_2 T^2 + C_3 T + C_4$$

**Table 3:** Parameters for reaction rate expressions.

Parameter	Value
$A_{WGS}$	$2.45 \times 10^2 \text{ mol}/(\text{bar kg}_{cat} \text{ s})$
$E_{act}$	$54.5 \times 10^3 \text{ J}/(\text{mol K})$
$C_1$	$1.760 \times 10^{-6} \text{ J}/(\text{mol K}^3)$
$C_2$	$-1.065 \times 10^{-2} \text{ J}/(\text{mol K}^2)$
$C_3$	$48.04 \text{ J}/(\text{mol K})$
$C_4$	$2.075 \times 10^2 \text{ J}/\text{mol}$

Extraction of hydrogen via the membrane should move the reaction away from equilibrium, towards the product side. The relative equilibrium ratio will be used to quantify the deviation from equilibrium (see equation 13). The addition of membranes to a fluidized bed is expected to significantly lower the local equilibrium ratio compared to a fluidized bed without membranes.

$$B_{WGS} = \frac{\left( \frac{P_{CO_2} P_{H_2}}{P_{CO} P_{H_2O}} \right)}{K_{eq,WGS}} \quad (13)$$

### Boundary conditions

All simulations have been performed with a 2D computational domain. For the gas mixture, a no-slip boundary condition was applied to the left and right walls, a constant gas velocity was imposed at the inlet, an imposed pressure condition was set at the outlet and the boundary condition of equation 12 was applied at the surface of the membranes. For the solids velocity and granular temperature, a Johnson & Jackson partial slip boundary condition with a specular coefficient of 0.50 was applied on the walls and the membranes (see Johnson et al. (1987)).

### Numerical schemes and accuracy

The temporal discretization was done with the second order Crank-Nicolson scheme. All simulations were run with an adjustable time-step, with a maximum time-step of  $1 \cdot 10^{-5}$  s. The time-step was selected each iteration based on a maximum Courant number of 0.1. A combination the second order Gauss linear and Van Leer scheme was used for the spatial discretization. The model's absolute tolerances for all quantities were within  $1 \cdot 10^{-11}$  each iteration.

## VERIFICATION, GEOMETRIES AND SETTINGS

### Reaction verification

The hydrodynamics and mass transfer parts of the model have been carefully verified and validated in our earlier works, see Medrano et al. (2015), Voncken et al. (2015) and Helmi et al. (2017). Gas flow profiles, packed bed pressure drop, convection-diffusion and diffusion only systems have all been verified with their respective analytical solutions. The fluidized bed's bubble properties and the membrane's hydrogen flux have been validated with experimental data. To verify whether the WGS reaction terms were implemented correctly, different types of basic reactions were compared to their analytical solutions. Furthermore, the WGS reaction has been simulated with the TFM and compared to a simple MATLAB numerical batch reactor model.

A first and second order reaction have been performed in a gas only batch reactor. The TFM mass fraction profiles in **Figure 1** match very well with the analytical solution. The mass fraction profiles for an equilibrium reaction with two species reacting to a product was also predicted correctly by the TFM (**Figure 2**).

The implementation of the WGS reaction rate equation was then checked by simulating a simple gas batch reactor system with the TFM, and comparing it with a gas batch reactor system in MATLAB. For this gas only verification study the catalyst efficiency for the WGS reaction was removed from the reaction rate equation.

**Figure 3** shows that the TFM results for WGS compares well with the gas batch reactor results obtained from the MATLAB code. These results verify that the TFM can be used to simulate various types of chemical reactions

and can predict the resulting concentration profiles accurately. To ensure equilibrium concentrations are correctly predicted by the TFM, the WGS verification simulation will be run for a longer period of time in future studies.

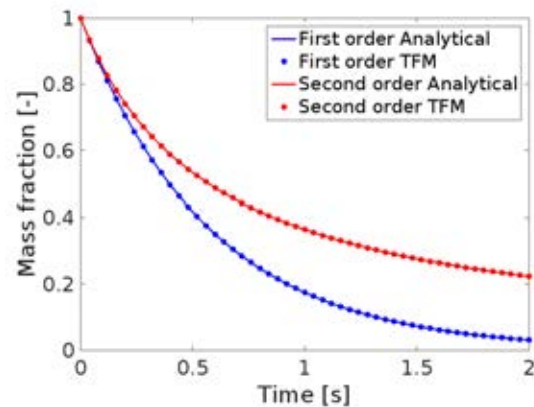


**Figure 1:** Analytical solution and TFM simulation result for a first and second order reaction.

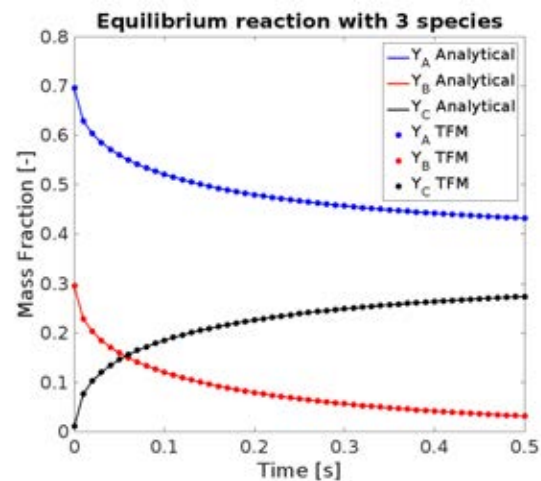


**Figure 2:** Analytical solution and TFM simulation result for a three species equilibrium reaction  $A + B \rightleftharpoons C$ .

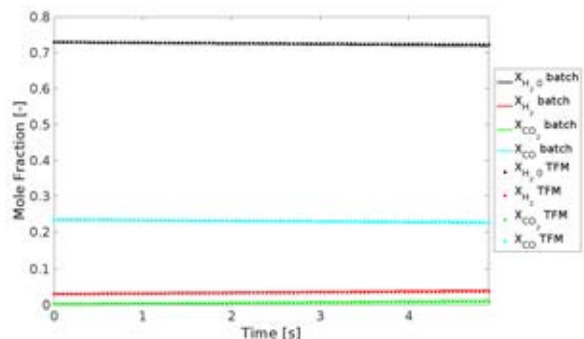


**Figure 3:** TFM simulation and batch reactor model comparison for the WGS reaction.

### Geometries and model settings

To quantify the effect of hydrogen extraction via a membrane on the reaction rate, systems with and without membranes were simulated. Both vertically and horizontally positioned membranes were looked into.

Fully 2D simulations have been performed. The geometries of all simulations are presented in **Table 4** and **Figure 4**. The horizontal membrane's diameter was set to 3.5 mm. Only one horizontal membrane has been simulated to show the effects that can occur in the system, in general, tube banks are best to be used to avoid hydrogen bypassing. The bed depths are only important for the calculation of the membrane area and do not hold any physical meaning in these 2D cases. The simulation settings can be found in **Table 5**. The vertical membrane was always placed at the left boundary. The horizontal membrane was placed at half of the reactor width.

**Table 4:** Geometries of all TFM WGS simulations.

Case	Width	Height	Depth
Vertical/no membrane	0.0356 m	0.0712 m	0.016 m
N <sub>cells</sub> vert./no memb.	40	80	-
Horizontal membrane	0.0356 m	0.0712 m	0.032 m
N <sub>cells</sub> horizontal memb.	40	80	-

**Table 5:** Summary of simulation settings for the WGS cases.

Quantity	Value	Unit
$d_p$	250	$\mu\text{m}$
$\rho_p$	1700	$\text{kg}/\text{m}^3$
$e_{pp}, e_{pw}$	0.97	-
$w/u_{mf}$	3	-
$D$	$1.0 \cdot 10^{-4}$	$\text{m}^2/\text{s}$
$Q_{pd}$	$4.3 \cdot 10^{-3}$	$\text{mol}/(\text{m}^2 \text{s Pa}^n)$
$n$	0.50	-
$T$	678	K
$X_{H_2}$	0.1	-
$X_{CH_4}$	0.1	-
$X_{H_2O}$	0.35	-
$X_{CO}$	0.35	-
$X_{CO_2}$	0.1	-
$\omega_{cat}$	0.10	-
$p_{outlet}$	3	bar
$p_{perm}$	$0.01 \cdot 10^5$	Pa
$t_{sim}$	10	s
$\Delta t$	$5 \cdot 10^{-6}$	s

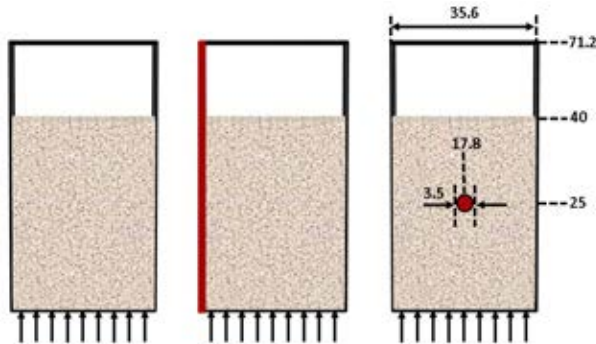


**Figure 4:** A fluidized bed: (left) without membranes; (middle) with a membrane at the left boundary; (right) with a horizontally immersed membrane. Dimensions are in mm.

## RESULTS

### Water Gas Shift

This section presents the results obtained by simulating fluidized beds with and without membranes in which the WGS reaction takes place. The reaction rate and equilibrium ratio will be used to assess the effect of the membrane on the system. The different types of membranes are not directly comparable, because they have different amount of hydrogen bypass and because the horizontal membrane affects the hydrodynamics. However, the effects that occur in these reactors can be described.

#### Reaction rate and equilibrium

The instantaneous and time-averaged reaction rates, and the time-averaged relative equilibrium ratio for a regular fluidized bed, fluidized bed with a vertical membrane and fluidized bed with a horizontal membrane are displayed in **Figure 5**. From the plot showing spatial distribution of the instantaneous reaction rates the position of the gas bubbles can be easily discerned as areas with reduced reaction rates related to the lower catalyst concentration inside the bubbles. The time-averaged reaction rates near the vertical membrane (the red line in the second row of **Figure 5**) are a factor 2 to 2.5 higher than the ones in a regular fluidized bed without membranes. The reaction is also further from its equilibrium state near the membrane than elsewhere in the reactor, which shows that the membrane flux is so high that kinetic and mass transfer limitations start to play a role.

Temporary gas pockets with low catalyst content occur underneath horizontally immersed membranes (Medrano et al. (2015)). Similar to bubbles, lower reaction rates are expected inside gas pockets compared to elsewhere in the reactor. This reduction in reaction rate is slightly visible in the time-averaged reaction rate plots for the horizontal membrane case. When the membrane tube is placed lower in the bed and closer to the wall the effect of gas pockets on a catalytic reaction rates is more pronounced (not shown). Contrary to the gas pockets, densified zones on top of the horizontal membrane increase the reaction rate locally with about a factor 4 to 5 compared to regular fluidized beds. However, despite the increased driving force, the hydrogen flux is still lowest on top of the horizontal membrane. Further investigation is required to quantify the mass transfer limitations in these densified zones and the effect of the position of the membranes in the bed.

#### Hydrogen concentrations and membrane geometry

**Figure 6** shows the hydrogen mole fraction profiles for a fluidized bed with a vertically and a horizontally immersed membrane. In both systems the membranes suffer from mass transfer limitations from the emulsion phase towards the membrane surface. Insufficient hydrogen is supplied to the membrane, so its flux is significantly lower than its maximum theoretical flux, which is referred to as concentration polarization. Caravella et al. (2009) and Helmi et al. (2017) have shown that concentration polarization are to be expected for systems with high flux membranes to extract one



chemical component from a gas mixture. Extraction of hydrogen increases the reaction rate and thus the hydrogen production. Clearly, the mass transfer rates of reactants and hydrogen towards the membrane is insufficient to maintain high hydrogen concentrations near the membrane, which are required to keep the driving force for permeation and the fluxes high. The differences in hydrogen mole fraction profiles clearly shows how differently vertically and horizontally

immersed membranes behave. The vertically immersed membrane is able to extract a large amount of hydrogen, hereby causing severe concentration polarization via a vertical concentration boundary layer. The underside of the horizontally immersed membranes is hardly limited by concentration polarization due to the direction of the gas flow, whereas the top has a high degree of concentration polarization, partially due to densified (defluidized) zones (see Voncken et al. (2015)).

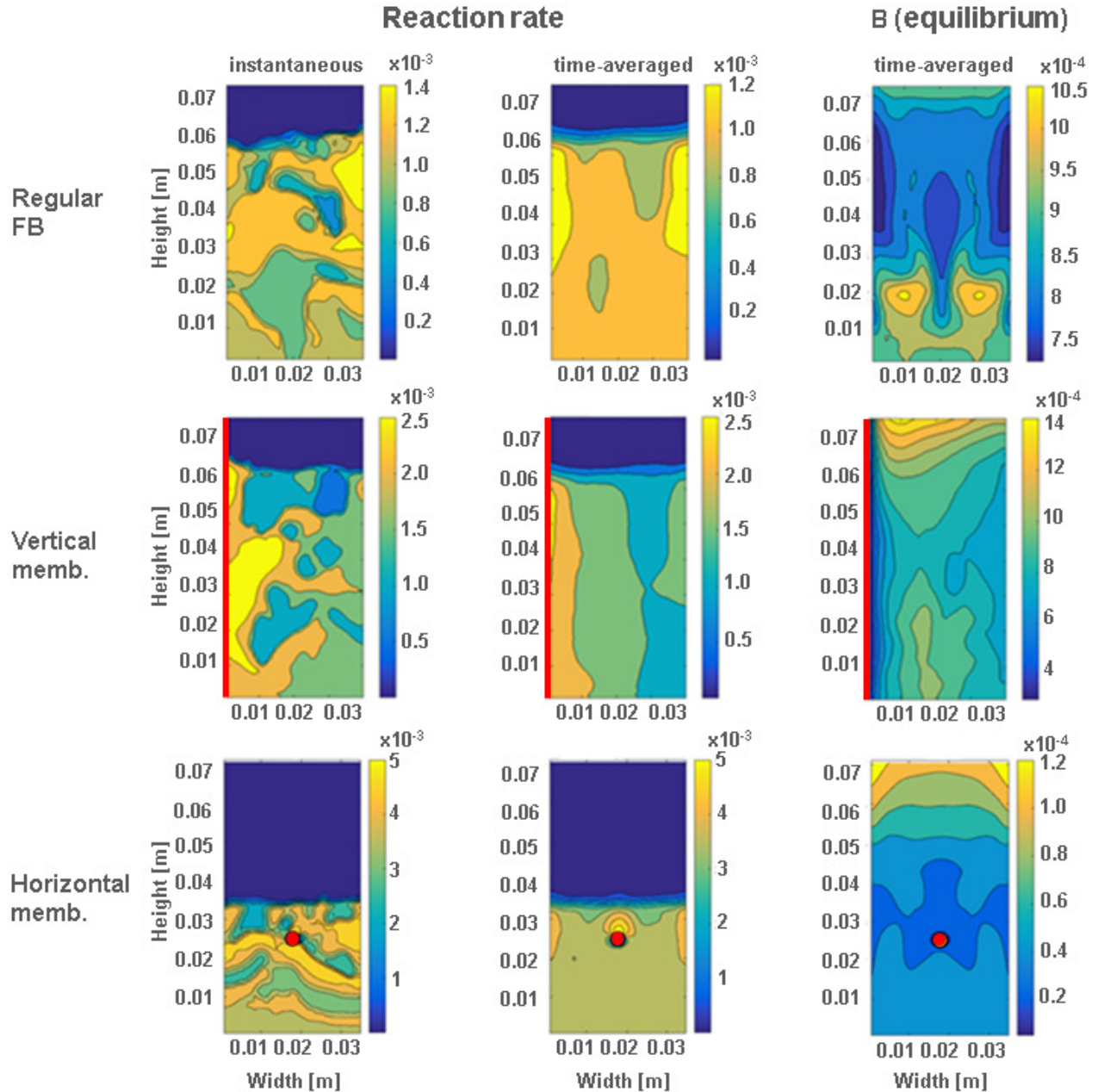


**Figure 5:** Instantaneous and time-averaged WGS reaction rates and time-averaged relative equilibrium ratio. Membranes are portrayed in red.

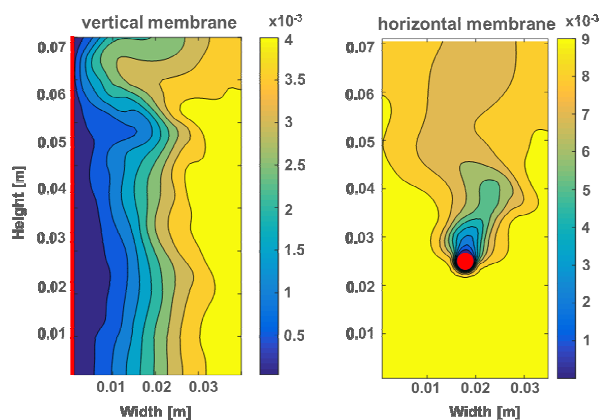


**Figure 6:** Hydrogen mole fraction profiles for fluidized bed reactors with a horizontally and vertically immersed membrane. The membranes are portrayed in red.

## CONCLUSION

A TFM with mass transfer, membranes and reactions was verified with various simple reactions such as  $n^{\text{th}}$  order, multi-species equilibrium reactions and Water Gas Shift. The verified TFM was then used to simulate WGS in fluidized beds without and with membranes. The membranes increase the reaction rate by a factor 2 to 5, depending on the geometry and orientation of the membrane. The extraction of hydrogen shifts the equilibrium of the reaction, especially in the vicinity of the membrane. For systems with vertically immersed membranes vertical mass transfer boundary layers develop, whereas for systems with horizontally immersed membranes, gas pockets with reduced reaction rates and densified zones with increased reaction rates prevail. Future studies will focus on the quantification of the concentration polarization effects and extend the investigations to Steam Methane Reforming.

## ACKNOWLEDGEMENTS

The authors are grateful to TTW and NWO for their financial support through the VIDI project ClingCO<sub>2</sub>, project number 12365. The authors thank Evert van Noort for his contribution to the simulation results.

## REFERENCES

- ADRI, A.M., LIM, C.J. and GRACE, J.R., (1994), "The fluidized bed membrane reactor system: a pilot scale experimental study", *Chem. Eng. Sc.*, **49**, 5833-5843.
- CARAVELLA, A., BARBIERI, G. and DRIOLI, E., (2009), "Concentration polarization analysis in self-supported Pd-based membranes", *Purif. Technol.*, **66**, 613-624.
- CORONEO, M., MONTANTE, G., CATALANO, J. and PAGLIANTI, A., (2009), "Modelling the effect of operating conditions on hydrodynamics and mass transfer in a Pd-Ag membrane module for H<sub>2</sub> purification", *J. Memb. Sc.*, **343**, 34-41.
- DANG, T.Y.N., KOLKMAN, T., GALLUCCI, F. and VAN SINT ANNALAND, M., (2013), "Development of a novel infrared technique for instantaneous, whole-

field, non invasive gas concentration measurements in gas-solid fluidized beds", *Chem. Eng. J.*, **219**, 545-557.

DE JONG, J.F., VAN SINT ANNALAND, M. and KUIPERS, J.A.M., (2012), "Membrane-assisted fluidized beds - part 2: numerical study on the hydrodynamics around immersed gas-permeating membrane", *Chem. Eng. Sc.*, **84**, 822-833.

ERGUN, S. and ORNING, A., (1949), "Fluid flow through randomly packed columns and fluidized beds", *Ind. Eng. Chem.*, **41**, 1179-1184.

FERNANDEZ, E., HELMI, A., COENEN, K., MELENDEZ, J., VIVIENTE, J.L., PACHECO TANAKA D.A., VAN SINT ANNALAND, M. and GALLUCCI, F., (2015), "Development of thin Pd-Ag supported membranes for fluidized bed membrane reactors including WGS related gases", *Int. J. Hydrogen Energy*, **40**, 3506-3519.

GALLUCCI, F., VAN SINT ANNALAND, M. and KUIPERS, J.A.M., (2008), "Autothermal reforming of methane with integrated CO<sub>2</sub> capture in a novel fluidized bed membrane reactor. Part 1: experimental demonstration", *Top. Catal.*, **51**, 133-145.

GIDASPOW, D., (1994), "Multiphase flow and fluidization: continuum and kinetic theory descriptions", *Academic Press Inc.*

HELMI, A., VONCKEN, R.J.W., RAIJMAKERS, T., ROGHAI, I., GALLUCCI, F., and VAN SINT ANNALAND, M., (2017), "On concentration polarization in fluidized bed membrane reactors", *Submitted to Chem. Eng. J.*

HOMMEL, R., Cloete, S. and AMINI, S., (2012), "Numerical investigations to quantify the effect of horizontal membranes on the performance of a fluidized bed reactor", *Int. J. Chem. React. Eng.*, **10**.

JOHNSON, P.C. and JACKSON, R., (1987), "Frictional-collisional constitutive relations for granular materials, with application to plane shearing", *J. Fluid Mech.*, **176**, 67-93.

KUIPERS, J.A.M., VAN DUIN, K.J., VAN BECKUM, F.P.H., and VAN SWAAIJ, W.P.M., (1992), "A numerical model of gas-fluidized beds", *Chem. Eng. Sc.*, **47**, 1913-1924.

LIU, Y. and HINRICHSEN, O., (2014), "CFD modeling of bubbling fluidized beds using OpenFOAM®: Model validation and comparison of TVD differencing schemes", *Comp. & Chem. Eng.*, **69**, 75-88.

LUN, C.K.K., SAVAGE, S.B., JEFFREY, D.J., and CHEPURNIY, N., (1984), "Kinetic theories for granular flow: inelastic particles in Couette flow and slightly inelastic particles in a general flowfield", *J. Fluid Mech.*, **140**, 223-256.

MA, D. and AHMADI, G., (1988), "A kinetic model for rapid granular flows of nearly elastic particles including interstitial fluid effects", *Powder Technol.*, **56**, 191-207.

MEDRANO, J.A., SPALLINA, V., VAN SINT ANNALAND, M. and GALLUCCI, F., (2014), "Thermodynamic analysis of a membrane-assisted chemical looping reforming reactor concept for combined H<sub>2</sub> production and CO<sub>2</sub> capture", *Int. J. Hydrogen Energy*, **39**, 4725-4738.



MEDRANO, J.A., VONCKEN, R.J.W., ROGHAI, I., GALLUCCI, F. and VAN SINT ANNALAND, M., (2015), "On the effect of gas pockets surrounding membranes in fluidized bed membrane reactors: An experimental and numerical study", *Chem. Eng. J.*, **282**, 45-57.

MLECZKO, L., OSTROWSKI, T. and WURZEL, T., (1996), "A fluidised-bed membrane reactor for the catalytic partial oxidation of methane to synthesis gas", *Chem. Eng. Sc.*, **51**, 3187-3192.

NIEUWLAND, J.J., VAN SINT ANNALAND, M., KUIPERS, J.A.M. and VAN SWAAIJ, W.P.M., (1996), "Hydrodynamic modeling of gas/particle flows in riser reactors", *AIChE J.*, **42**, 1569-1582.

NUMAGUCHI, T. and KUKUCHI, K., (1988), "Intrinsic kinetics and design simulation in a complex reaction network: Steam-Methane Reforming", *Chem. Eng. Sc.*, **43**, 2295-2301.

PASSALACQUA, A. and FOX, R.O., (2011), "Implementation of an iterative solution procedure for multi-fluid gas-particle flow models on unstructured grids", *Powder Technol.*, **213**, 174-187.

PATIL, C.S., VAN SINT ANNALAND, M. and KUIPERS, J.A.M., (2007), "Fluidised bed membrane reactor for ultrapure hydrogen production via methane steam reforming: Experimental demonstration and model validation", *Chem. Eng. Sci.*, **62**, 2989-3007.

RUSCHE, H., (2002), "Computational fluid dynamics of dispersed two-phase flows at high phase fractions", PhD thesis, *University of London*.

SRIVASTAVA, A. and SUNDARESAN, S., (2003), "Analysis of a frictional-kinetic model for gas-particle flow", *Powder Technol.*, **129**, 72-85.

TAN, L., ROGHAI, I. and VAN SINT ANNALAND, M., (2014), "Simulation study on the effect of gas permeation on the hydrodynamic characteristics of membrane-assisted micro fluidized beds", *Appl. Math. Model.*, **38**, 4291-4307.

TIEMERSMA, T.P., PATIL, C.S., VAN SINT ANNALAND, M. and KUIPERS, J.A.M., (2006), "Modelling of packed bed membrane reactors for autothermal production of ultrapure hydrogen", *Chem. Eng. Sc.*, **61**, 1602-1616.

VAN DER HOEF, M.A., YE, M., VAN SINT ANNALAND, M., ANDREWS IV, A.T., SUNDARESAN, S. and KUIPERS, J.A.M., (2006) "Multi-scale modeling of gas-fluidized beds", *Adv. Chem. Eng.* **31**, 65-149.

VAN WACHEM, B.G.M., (2000), "Derivation, implementation, and validation of computer simulation models for gas-solid fluidized beds", PhD thesis, Delft University of Technology.

VONCKEN, R., ROGHAI, I., GALLUCCI, F. and VAN SINT ANNALAND, M., (2015), "Mass transfer phenomena in fluidized beds with vertically and horizontally immersed membranes", *Proc. 11th Int. Conf. Comput. Fluid Dyn. Miner. Process Ind. (CFD 2015)*, 031VON 1-6.

WEN, C. and YU, Y., (1966) "A generalized method for predicting the minimum fluidization velocity" *AIChEJ.* **12**, 610-612.